Inverse medium scattering for the Helmholtz equation at fixed frequency

Gang Bao and Peijun Li

Department of Mathematics, Michigan State University, East Lansing, MI 48824-1027, USA

E-mail: bao@math.msu.edu and lipeijun@math.msu.edu

Abstract

Consider a time-harmonic electromagnetic plane wave incident on a medium enclosed by a bounded domain in $\mathbb{R}^2$. In this paper, existence and uniqueness of the variational problem for the direct scattering are established. An energy estimate for the scattered field is obtained on which the Born approximation is based. The Fréchet differentiability of the scattering map is examined. A new continuation method for the inverse medium scattering, which reconstructs the scatterer of an inhomogeneous medium from the boundary measurements of the scattered waves, is developed. The algorithm requires only single-frequency scattering data. Using an initial guess from the Born approximation, each update is obtained via recursive linearization on the spatial frequency of a one-parameter family of plane waves by solving one forward and one adjoint problem of the Helmholtz equation.

(Some figures in this article are in colour only in the electronic version)

1. Introduction

Consider the Helmholtz equation in two dimensions

$$\Delta\phi + k_0^2(1 + q(x))\phi = 0, \tag{1.1}$$

where ϕ is the total field, k_0 is the wavenumber, and $q(x) > -1$, which has a compact support and a lower bound, is the scatterer.

Assume that the scatterer lies in the upper half plane $\mathbb{R}_+^2 = \{(x_1, x_2) \in \mathbb{R}^2 : x_2 > 0\}$. Denote the wave vector $\mathbf{k} = (\eta, k(\eta))$, where η is the transverse part of the wave vector and

$$k(\eta) = \begin{cases} \sqrt{k_0^2 - \eta^2}, & \text{for } k_0 \geqslant |\eta|, \\ \mathrm{i}\sqrt{\eta^2 - k_0^2}, & \text{for } k_0 < |\eta|. \end{cases}$$

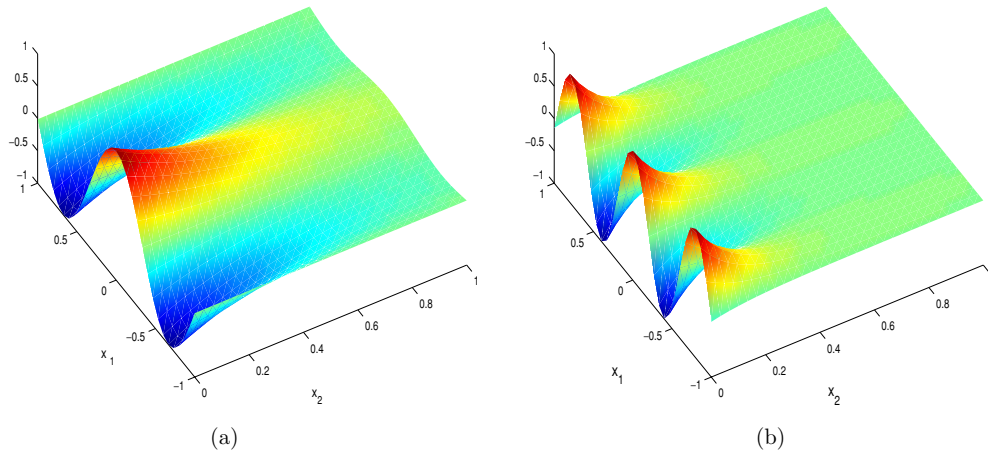The number $|\eta|$ is known as the spatial frequency.

Figure 1. Evanescent plane wave at $k_0 = 4.0$: (a) $\eta = 4.7$ and (b) $\eta = 8.0$.

The scatterer is illuminated by a one-parameter family of plane waves

$$\phi_0 = e^{i\mathbf{k} \cdot x}, \tag{1.2}$$

which gives explicitly

$$\phi_0(x_1, x_2) = \begin{cases} \exp\left(i\left(\eta x_1 + \sqrt{k_0^2 - \eta^2} x_2\right)\right), & \text{for} \quad k_0 \geqslant |\eta|, \\ \exp\left(i\eta x_1 - \sqrt{\eta^2 - k_0^2} x_2\right), & \text{for} \quad k_0 < |\eta|. \end{cases}$$

The modes for which $|\eta| \leqslant k_0$ correspond to propagating plane waves while the modes with $|\eta| > k_0$ correspond to evanescent plane waves. Therefore, the illuminating field could consist of high spatial frequency evanescent plane waves. They may be generated at the interface of two media by total internal reflection [10, 13], which has been in practical use for decades and primarily been used in near-field optics [4, 5]. A recent review on the near-field microscopy and near-field optics may be found in [9]. These waves are oscillatory parallel to the x_1 axis and decay exponentially along the x_2 axis in the upper half plane $\mathbb{R}_+^2$. The higher the spatial frequency of the evanescent plane waves used to probe the scatterer, the more rapidly the field decays as a function of depth into the scatterer. See figure 1 for an example. Evidently, such incident waves satisfy the homogeneous equation

$$\Delta \phi_0 + k_0^2 \phi_0 = 0. \tag{1.3}$$

The total electric field ϕ consists of the incident field ϕ_0 and the scattered field ψ:

$$\phi = \phi_0 + \psi.$$

It follows from equations (1.1) and (1.3) that the scattered field satisfies

$$\Delta \psi + k_0^2 (1 + q) \psi = -k_0^2 q \phi_0. \tag{1.4}$$

Remark 1.1. In this paper, we adopt the non-global approach, i.e., the scattered field resulting from the interaction of the incident field with the scatterer is analysed in the absence of any other medium or tip. The scattering problem may be formulated in the free space. The global approach which takes into account the entire system is the subject of our ongoing research.

In the free space, the scattered field is required to satisfy the following Sommerfeld radiation condition:

$$\lim_{r \to \infty} \sqrt{r} \left(\frac{\partial \psi}{\partial r} - \mathrm{i}k_0 \psi \right) = 0, \qquad r = |x|,$$

uniformly along all directions $x/|x|$. In practice, it is convenient to reduce the problem to a bounded domain by introducing an artificial surface. Let $D = [-L_1, L_1] \times [0, L_2]$ be a square which contains the compact support of the scatterer, Ω. Let ∂D be the boundary of D. Denote by n the unit outward normal to ∂D. A suitable boundary condition needs to be imposed on ∂D. For the sake of simplicity, we employ the first-order absorbing boundary condition [15] as

$$\frac{\partial \psi}{\partial n} - \mathrm{i}k_0 \psi = 0, \qquad \text{on} \qquad \partial D. \tag{1.5}$$

Given the incident field ϕ_0, the direct problem is to determine the scattered field ψ for the known scatterer $q(x)$. Using the Lax–Milgram lemma and the Fredholm alternative, the direct problem is shown in this paper to have a unique solution for all $k_0 > 0$. An energy estimate for the scattered field is given, which provides a criterion for the weak scattering. Furthermore, properties on the continuity and the Fréchet differentiability of the nonlinear scattering map are examined. For the regularity analysis of the scattering map in an open domain, the reader is referred to [1, 8, 16]. The inverse medium scattering problem is to determine the scatterer $q(x)$ from the measurements of near-field currents densities, $\psi|_{\partial D}$, given the incident field ϕ_0. The inverse medium scattering problems arise naturally in diverse applications such as radar, sonar, geophysical exploration, medical imaging and nondestructive testing [8]. However, there are two major difficulties associated with these inverse problems: the ill-posedness and the presence of many local minima. In [3, 6], stable and efficient continuation methods with respect to the wavenumber were proposed to solve the two-dimensional Helmholtz equation and the three-dimensional Maxwell's equations, respectively, in the case of full aperture data. A homotopy continuation method with limited aperture data may be found in [2]. These approaches require multi-frequency scattering data and are based on recursive linearization along wavenumbers.

The main purpose of this paper is to study the inverse medium problem for Helmholtz's equations at a single frequency. We present a new continuation method for the inverse medium scattering problem. In the case of radially symmetric scatterers, Chen [7] developed a recursive linearization algorithm with single-frequency data, where spherical incident waves were used. In this paper, we attempt to remove the radially symmetric assumption on the medium. Our approach is motivated by the recent studies of near-field optics. As a special feature, the illuminating fields used in this paper including the high spatial frequency evanescent plane waves are a one-parameter family of plane waves. When a medium is probed with an evanescent plane wave at a high spatial frequency, only a thin layer of the medium is penetrated. Corresponding to this exponentially decaying incident field, the scattered field measured on the boundary contains information of the medium in that thin layer. Although such a measurement is entirely inadequate to determine the whole medium, it does give rise to an approximation. To accurately determine the medium, information at lower spatial frequencies of the evanescent plane waves is needed to illuminate the medium. While the probing field penetrates a thicker layer of the medium, the relation between the measurement and the scatterer to be recovered in the thicker layer becomes more nonlinear. These nonlinear equations can be considered as perturbations to the already solved equations in the previous thicker layers. Therefore, they can be continually and recursively linearized by a standard perturbation technique. Thus, the recursive linearization is a continuation method along the transverse direction of the incident wave, which controls the depth of its penetration.

The plan of this paper is as follows. The analysis of the variational problem for direct scattering is presented is section 2. In particular, the well-posedness of the direct scattering is proved. The Fréchet differentiability of the scattering map is also given. In section 3, an initial guess of the reconstruction from the Born approximation is derived in the case of weak scattering. Section 4 is devoted to numerical study of a regularized iterative linearization algorithm. Numerical examples are presented. The paper is concluded with some general remarks and directions for future research in section 5.

2. Analysis of the scattering map

In this section, the direct scattering problem is studied to provide some criterion for the weak scattering, which plays an important role in the inversion method. The Fréchet differentiability of the scattering map for the problem (1.4), (1.5) is examined.

Remark 2.1. Some analysis of the scattering map was given previously by Keys and Weglein [16] based on the integral equation approach and contraction mapping theorem. The assumption of small perturbation of the potential is necessary for their approach. Our approach is different. Based on the Fredholm alternative and a uniqueness result, we develop a variational approach to prove the existence of the scattered field for all $k_0 > 0$, given $q \in L^\infty(D)$, the continuity of the scattering map, the boundedness of the formal linearized map and the Fréchet differentiability of the scattering map. The assumption of small perturbation is not needed in our analysis. More importantly, we give an explicit energy estimate for the scattered field, which provides a criterion for weak scattering hence plays a central role in the development of the inversion algorithm of section 3. An analysis of the Fréchet differentiability on the scattering map for equation (1.4) along with the Sommerfeld radiation condition may also be found in [1] using the integral equation approach.

To state our boundary value problem, we introduce the bilinear form $a: H^1(D) \times H^1(D) \to \mathbb{C}$

$$a(u, v) = (\nabla u, \nabla v) - k_0^2((1 + q)u, v) - ik_0\langle u, v\rangle,$$

and the linear functional on $H^1(D)$

$$b(v) = k_0^2(q\phi_0, v).$$

Here, we have used the standard inner products

$$(u, v) = \int_D u \cdot \overline{v} \, dx \qquad \text{and} \qquad \langle u, v\rangle = \int_{\partial D} u \cdot \overline{v} \, ds,$$

where the overline denotes the complex conjugate.

Then, we have the weak form of the boundary value problem (1.4) and (1.5): to find $\psi \in H^1(D)$ such that

$$a(\psi, \xi) = b(\xi), \qquad \forall \, \xi \in H^1(D). \tag{2.1}$$

Throughout the paper, the constant C stands for a positive generic constant whose value may change step by step, but should always be clear from the context.

For a given scatterer q and an incident field ϕ_0, we define the map $S(q, \phi_0)$ by $\psi = S(q, \phi_0)$, where ψ is the solution of the problem (1.4), (1.5) or the variational problem (2.1). It is easily seen that the map $S(q, \phi_0)$ is linear with respect to ϕ_0 but is nonlinear with respect to q. Hence, we may denote $S(q, \phi_0)$ by $S(q)\phi_0$.

Concerning the map $S(q)$, we have the following regularity results. Lemma 2.3 gives the boundedness of $S(q)$, while a continuity result for the map $S(q)$ is presented in lemma 2.4.

Lemma 2.1. *Given the scatterer $q \in L^{\infty}(D)$, the direct scattering problem (1.4), (1.5) has at most one solution.*

Proof. It suffices to show that $\psi = 0$ in D if $\phi_0 = 0$ (no source term). From the Green's formula

$$0 = \int_D (\psi \Delta \overline{\psi} - \overline{\psi} \Delta \psi) \, \mathrm{d}x = \int_{\partial D} \left(\psi \frac{\partial \overline{\psi}}{\partial n} - \overline{\psi} \frac{\partial \psi}{\partial n} \right) \mathrm{d}s = -2\mathrm{i}k_0 \int_{\partial D} |\psi|^2 \, \mathrm{d}s,$$

we get $\psi = 0$ on ∂D. The absorbing boundary condition on ∂D yields further that $\frac{\partial \psi}{\partial n} = 0$ on ∂D. By the Holmgren uniqueness theorem, $\psi = 0$ in $\mathbb{R}^2 \backslash D$. A unique continuation result [14] concludes that $\psi = 0$ in D. $\qquad\square$

Lemma 2.2. *If the wavenumber k_0 is sufficiently small, the variational problem (2.1) admits a unique weak solution in $H^1(D)$ and $S(q)$ is a bounded linear map from $L^2(D)$ to $H^1(D)$. Furthermore, there is a constant C dependent on D, such that*

$$\|S(q)\phi_0\|_{H^1(D)} \leqslant Ck_0 \|q\|_{L^{\infty}(D)} \|\phi_0\|_{L^2(D)}. \tag{2.2}$$

Proof. Decompose the bilinear form a into $a = a_1 + k_0^2 a_2$, where

$$a_1(\psi, \xi) = (\nabla \psi, \nabla \xi) - \mathrm{i}k_0 \langle \psi, \xi \rangle, \qquad a_2(\psi, \xi) = -((1+q)\psi, \xi).$$

We conclude that a_1 is coercive from

$$\begin{aligned} |a_1(\psi, \psi)| &\geqslant C \big(\|\nabla \psi\|_{L^2(D)}^2 + k_0 \|\psi\|_{H^{1/2}(\partial D)}^2 \big) \\ &\geqslant Ck_0 \big(\|\nabla \psi\|_{L^2(D)}^2 + \|\psi\|_{H^{1/2}(\partial D)}^2 \big) \\ &\geqslant Ck_0 \|\psi\|_{H^1(D)}^2, \end{aligned}$$

where the last inequality may be obtained by applying standard elliptic estimates [12]. Next, we prove the compactness of a_2. Define an operator $\mathcal{A}: L^2(D) \to H^1(D)$ by

$$a_1(\mathcal{A}\psi, \xi) = a_2(\psi, \xi), \qquad \forall \, \xi \in H^1(D),$$

which gives

$$(\nabla \mathcal{A}\psi, \nabla \xi) - \mathrm{i}k_0 \langle \mathcal{A}\psi, \xi \rangle = -((1+q)\psi, \xi), \qquad \forall \, \xi \in H^1(D).$$

Using the Lax–Milgram lemma, it follows that

$$\|\mathcal{A}\psi\|_{H^1(D)} \leqslant \frac{C}{k_0} \|\psi\|_{L^2(D)}, \tag{2.3}$$

where the constant C is independent of k_0. Thus, $\mathcal{A}$ is bounded from $L^2(D)$ to $H^1(D)$ and $H^1(D)$ is compactly imbedded into $L^2(D)$. Hence, $\mathcal{A}: L^2(D) \to L^2(D)$ is a compact operator.

Define a function $u \in L^2(D)$ by requiring $u \in H^1(D)$ and satisfying

$$a_1(u, \xi) = b(\xi), \qquad \forall \, \xi \in H^1(D).$$

It follows from the Lax–Milgram lemma again that

$$\|u\|_{H^1(D)} \leqslant Ck_0 \|q\|_{L^{\infty}(D)} \|\phi_0\|_{L^2(D)}. \tag{2.4}$$

Using the operator $\mathcal{A}$, we can see that the problem (2.1) is equivalent to find $\psi \in L^2(D)$ such that

$$(\mathcal{I} + k_0^2 \mathcal{A})\psi = u. \tag{2.5}$$

When the wavenumber k_0 is small enough, the operator $\mathcal{I} + k_0^2\mathcal{A}$ has a uniformly bounded inverse. We then have the estimate

$$\|\psi\|_{L^2(D)} \leqslant C\|u\|_{L^2(D)}, \tag{2.6}$$

where the constant C is independent of k_0. Rearranging (2.5), we have $\psi = u - k_0^2\mathcal{A}\psi$, so $\psi \in H^1(D)$ and, by the estimate (2.3) for the operator $\mathcal{A}$, we have

$$\|\psi\|_{H^1(D)} \leqslant \|u\|_{H^1(D)} + Ck_0\|\psi\|_{L^2(D)}.$$

The proof is complete by combining the estimates (2.6) and (2.4) and observing that $\psi = S(q)\phi_0$. □

For a general wavenumber $k_0 > 0$, from equation (2.5), the existence follows from the Fredholm alternative and the uniqueness result. However, the constant C in the estimate (2.2) depends on the wavenumber.

Lemma 2.3. *Given the scatterer $q \in L^\infty(D)$, the variational problem (2.1) admits a unique weak solution in $H^1(D)$ for all $k_0 > 0$ and $S(q)$ is a bounded linear map from $L^2(D)$ to $H^1(D)$. Furthermore, the estimate*

$$\|S(q)\phi_0\|_{H^1(D)} \leqslant C\|q\|_{L^\infty(D)}\|\phi_0\|_{L^2(D)}, \tag{2.7}$$

holds, where the constant C depends on k_0 and D.

Remark 2.2. It follows from the explicit form of the incident field (1.2) and the estimate (2.7) that

$$\|\psi\|_{H^1(D)} \leqslant C|\Omega|^{\frac{1}{2}}\|q\|_{L^\infty(D)},$$

where Ω is the compact support of the scatterer q and the constant C depends on k_0, D. Moreover, we have for $|\eta| > k_0$ that

$$\|\psi\|_{H^1(D)} \leqslant C(\eta^2 - k_0^2)^{-1/4}\|q\|_{L^\infty(D)}, \tag{2.8}$$

where the constant C depends on k_0 and D.

Remark 2.3. The estimate of the scattered field in remark 2.1 provides a criterion for the weak scattering. For a fixed wavenumber k_0 and a scatterer q, the scattered field is weak if the spatial frequency of the incident wave, $|\eta|$, is large.

Lemma 2.4. *Assume that $q_1, q_2 \in L^\infty(D)$. Then,*

$$\|S(q_1)\phi_0 - S(q_2)\phi_0\|_{H^1(D)} \leqslant C\|q_1 - q_2\|_{L^\infty(D)}\|\phi_0\|_{L^2(D)}, \tag{2.9}$$

where the constant C depends on k_0, D and $\|q_2\|_{L^\infty(D)}$.

Proof. Let $\psi_1 = S(q_1)\phi_0$ and $\psi_2 = S(q_2)\phi_0$. It follows that for $j = 1, 2$

$$\Delta\psi_j + k_0^2(1 + q_j)\psi_j = -k_0^2 q_j\phi_0.$$

By setting $w = \psi_1 - \psi_2$, we have

$$\Delta w + k_0^2(1 + q_1)w = -k_0^2(q_1 - q_2)(\phi_0 + \psi_2).$$

The function w also satisfies the boundary condition (1.5).

We repeat the procedure in the proof of lemma 2.3 to obtain

$$\|w\|_{H^1(D)} \leqslant C\|q_1 - q_2\|_{L^\infty(D)}\|\phi_0 + \psi_2\|_{L^2(D)}.$$

Using lemma 2.3 again for ψ_2 yields

$$\|\psi_2\|_{H^1(D)} \leqslant C\|q_2\|_{L^\infty(D)}\|\phi_0\|_{L^2(D)},$$

which gives

$$\|S(q_1)\phi_0 - S(q_2)\phi_0\|_{H^1(D)} \leqslant C\|q_1 - q_2\|_{L^\infty(D)}\|\phi_0\|_{L^2(D)},$$

where the constant C depends on D, k_0 and $\|q_2\|_{L^\infty(D)}$. $\qquad\qquad\qquad\square$

Let γ be the restriction (trace) operator to the boundary ∂D. By the trace theorem, γ is a bounded linear operator from $H^1(D)$ onto $H^{1/2}(\partial D)$. We can now define the scattering map $M(q) = \gamma S(q)$.

Next, consider the Fréchet differentiability of the scattering map. Recall the map $S(q)$ is nonlinear with respect to q. Formally, by using the first-order perturbation theory, we obtain the linearized scattering problem of (1.4), (1.5) with respect to a reference scatterer q,

$$\Delta v + k_0^2(1 + q)v = -k_0^2\delta q(\phi_0 + \psi), \tag{2.10}$$

$$\frac{\partial v}{\partial n} - ik_0 v = 0, \tag{2.11}$$

where $\psi = S(q)\phi_0$.

Define the formal linearization $T(q)$ of the map $S(q)$ by $v = T(q)(\delta q, \phi_0)$, where v is the solution of the problem (2.10), (2.11). The following is a boundedness result for the map $T(q)$. A proof may be given by following step by step the proofs of lemmas 2.2 and 2.3. Hence, we omit it here.

Lemma 2.5. *Assume that* $q, \delta q \in L^\infty(D)$ *and* ϕ_0 *is the incident field. Then* $v = T(q)(\delta q, \phi_0) \in H^1(D)$ *with the estimate*

$$\|T(q)(\delta q, \phi_0)\|_{H^1(D)} \leqslant C\|\delta q\|_{L^\infty(D)}\|\phi_0\|_{L^2(D)}, \tag{2.12}$$

where the constant C *depends on* k_0, D *and* $\|q\|_{L^\infty(D)}$.

The next lemma is concerned with the continuity property of the map.

Lemma 2.6. *For any* $q_1, q_2 \in L^\infty(D)$ *and an incident field* ϕ_0, *the following estimate holds:*

$$\|T(q_1)(\delta q, \phi_0) - T(q_2)(\delta q, \phi_0)\|_{H^1(D)} \leqslant C\|q_1 - q_2\|_{L^\infty(D)}\|\delta q\|_{L^\infty(D)}\|\phi_0\|_{L^2(D)}, \tag{2.13}$$

where the constant C *depends on* k_0, D *and* $\|q_2\|_{L^\infty(D)}$.

Proof. Let $v_i = T(q_i)(\delta q, \phi_0)$, for $i = 1, 2$. It is easy to see that

$$\Delta(v_1 - v_2) + k_0^2(1 + q_1)(v_1 - v_2) = -k_0^2\delta q(\psi_1 - \psi_2) - k_0^2(q_1 - q_2)v_2,$$

where $\psi_i = S(q_i)\phi_0$.

Similar to the proof of lemma 2.3, we get

$$\|v_1 - v_2\|_{H^1(D)} \leqslant C(\|\delta q\|_{L^\infty(D)}\|\psi_1 - \psi_2\|_{H^1(D)} + \|q_1 - q_2\|_{L^\infty(D)}\|v_2\|_{H^1(D)}).$$

From lemmas 2.2 and 2.3, we obtain

$$\|v_1 - v_2\|_{H^1(D)} \leqslant C\|q_1 - q_2\|_{L^\infty(D)}\|\delta q\|_{L^\infty(D)}\|\phi_0\|_{L^2(D)},$$

which completes the proof. $\qquad\qquad\qquad\square$

The following result concerns the differentiability property of $S(q)$.

Lemma 2.7. *Assume that* $q, \delta q \in L^\infty(D)$. *Then there is a constant* C *dependent on* k_0, D *and* $\|q\|_{L^\infty(D)}$, *for which the following estimate holds:*

$$\|S(q + \delta q)\phi_0 - S(q)\phi_0 - T(q)(\delta q, \phi_0)\|_{H^1(D)} \leqslant C\|\delta q\|_{L^\infty(D)}^2\|\phi_0\|_{L^2(D)}. \tag{2.14}$$

Proof. By setting $\psi_1 = S(q)\phi_0$, $\psi_2 = S(q+\delta q)\phi_0$ and $v = T(q)(\delta q, \phi_0)$, we have

$$\Delta\psi_1 + k_0^2(1+q)\psi_1 = -k_0^2 q\phi_0,$$
$$\Delta\psi_2 + k_0^2(1+q+\delta q)\psi_2 = -k_0^2(q+\delta q)\phi_0,$$
$$\Delta v + k_0^2(1+q)v = -k_0^2\delta q\psi_1 - k_0^2\delta q\phi_0.$$

In addition, ψ_1, ψ_2 and v satisfy the boundary condition (1.5).

Denote $U = \psi_2 - \psi_1 - v$. Then,

$$\Delta U + k_0^2(1+q)U = -k_0^2\delta q(\psi_2 - \psi_1).$$

Similar arguments as in the proof of lemma 2.3 give

$$\|U\|_{H^1(D)} \leqslant C\|\delta q\|_{L^\infty(D)}\|\psi_2 - \psi_1\|_{H^1(D)}.$$

From lemma 2.3, we obtain further that

$$\|U\|_{H^1(D)} \leqslant C\|\delta q\|_{L^\infty(D)}^2\|\phi_0\|_{L^2(D)}.$$

Finally, by combining the above lemmas, we arrive at $\square$

Theorem 2.1. *The scattering map $M(q)$ is Fréchet differentiable with respect to q and its Fréchet derivative is*

$$DM(q) = \gamma T(q). \tag{2.15}$$

3. Inverse medium scattering

In this section, a regularized recursive linearization method for solving the inverse medium scattering problem of the Helmholtz equation in two dimensions is proposed. The algorithm, obtained by a continuation method on the spatial frequency of a one-parameter family of incident plane waves, requires only single-frequency scattering data. At each transverse part of the incident wave, the algorithm determines a forward model which produces the prescribed scattering data. Since the incident wave at a high spatial frequency can only penetrate a thin layer of the scatterer, the scattered field is weak. Consequently, the nonlinear equation becomes essentially linear, known as the Born approximation. The algorithm first solves this nearly linear equation at the largest $|\eta|$ to obtain an approximation of the scatterer. This approximation is then used to linearize the nonlinear equation at the next smaller spatial frequency of the incident wave, which can penetrate a thicker layer of the scatterer, to produce a better approximation. When the spatial frequency, $|\eta|$, is smaller than the fixed wavenumber k_0, the incident wave becomes usual propagating plane wave and the whole scatterer is illuminated. This process is continued until the spatial frequency is zero, where the approximation of the scatterer is considered as the final reconstruction.

3.1. Born approximation

Rewrite (1.4) as

$$\Delta\psi + k_0^2\psi = -k_0^2 q(\phi_0 + \psi). \tag{3.1}$$

Consider a test function $\psi_0 = e^{ik_0 x \cdot \vec{d}}$, $\vec{d} = (\cos\theta, \sin\theta)$, $\theta \in [0, 2\pi]$. Hence, ψ_0 satisfies (1.3).

Multiplying equation (3.1) by ψ_0 and integrating over D on both sides, we have

$$\int_D \psi_0\Delta\psi\,\mathrm{d}x + k_0^2\int_D \psi_0\psi\,\mathrm{d}x = -k_0^2\int_D q(\phi_0 + \psi)\psi_0\,\mathrm{d}x.$$

Integration by parts yields

$$\int_D \psi \Delta \psi_0 \, dx + \int_{\partial D} \left(\psi_0 \frac{\partial \psi}{\partial n} - \psi \frac{\partial \psi_0}{\partial n} \right) ds + k_0^2 \int_D \psi_0 \psi \, dx = -k_0^2 \int_D q(\phi_0 + \psi) \psi_0 \, dx.$$

We have by noting (1.3) and the boundary condition (1.5) that

$$\int_D q(\phi_0 + \psi) \psi_0 \, dx = \frac{1}{k_0^2} \int_{\partial D} \psi \left(\frac{\partial \psi_0}{\partial n} - ik_0 \psi_0 \right) ds.$$

Using the special form of the incident wave and the test function, we then get

$$\int_D q(x) \exp(i(\eta + k_0 \cos \theta)x_1) \exp(i(k(\eta) + k_0 \sin \theta)x_2) \, dx$$
$$= \frac{i}{k_0} \int_{\partial D} \psi (n \cdot \vec{d} - 1) \, e^{ik_0 x \cdot \vec{d}} \, ds - \int_D q \psi \psi_0 \, dx. \qquad (3.2)$$

From lemma 2.3 and remark 2.2, using an evanescent incident plane wave at a high spatial frequency, the scattered field is weak and the inverse scattering problem becomes essentially linear. Dropping the nonlinear (second) term of (3.2), we obtain the linearized integral equation

$$\int_D q(x) \exp i(\eta + k_0 \cos \theta)x_1 \exp \left(\left(-\sqrt{\eta^2 - k_0^2} + ik_0 \sin \theta \right)x_2 \right) dx$$
$$= \frac{i}{k_0} \int_{\partial D} \psi (n \cdot \vec{d} - 1) \, e^{ik_0 x \cdot \vec{d}} \, ds, \qquad (3.3)$$

which is the Born approximation.

Since the scatterer $q(x)$ has a compact support, (3.3) can be rewritten as

$$\int_0^{L_2} \hat{q}(\xi, x_2) \exp\left(\left(-\sqrt{\eta^2 - k_0^2} + ik_0 \sin \theta \right)x_2 \right) dx_2 = \frac{i}{k_0} \int_{\partial D} \psi (n \cdot \vec{d} - 1) \, e^{ikx \cdot \vec{d}} \, ds,$$

where $\xi = \eta + k_0 \cos \theta$ and $\hat{q}(\xi, x_2)$ is the Fourier transform of $q(x)$ with respect to x_1. When the spatial frequency $|\eta|$ is large, the incident wave penetrates a thin layer of the scatterer. Thus, the Born approximation allows a reconstruction containing information of the true scatterer in that thin layer. In [6, 3], the inversion involves data related to the scatterer through the Fourier transform in the case of weak scattering. Here, due to the presence of the evanescent wave, the inversion involves data related to the scatterer through a Fourier (with respect to x_1)–Laplace (with respect to x_2) transform in the case of the weak scattering. Since the inversion of the Laplace transform is ill-posed, we consider the Landweber iteration to implement the linear integral equation (3.3) in order to reduce the computation cost and instability [17].

Define the data

$$f(\eta, \theta) = \begin{cases} \dfrac{i}{k_0} \displaystyle\int_{\partial D} \psi (n \cdot \vec{d} - 1) \, e^{ikx \cdot \vec{d}} \, ds, & \text{for} \quad |\eta| \geqslant \eta_{max}, \\ 0, & \text{for} \quad |\eta| < \eta_{max}, \end{cases}$$

where η_{max} is some large positive number.

The integral equation (3.3) can be written as the operator form

$$A(\eta, \theta; x)q(x) = f(\eta, \theta). \qquad (3.4)$$

Following the idea of the Kaczmarz method, we use partial measurement data instead of using all them simultaneously for each sweep. Let $\eta_i, i = 1, \ldots, I$, be the discretization of η, where I is the number of sweeps. Then, we can rewrite (3.4) as

$$A(\eta_i, \theta; x)q(x) = f(\eta_i, \theta), \qquad i = 1, \ldots, I,$$
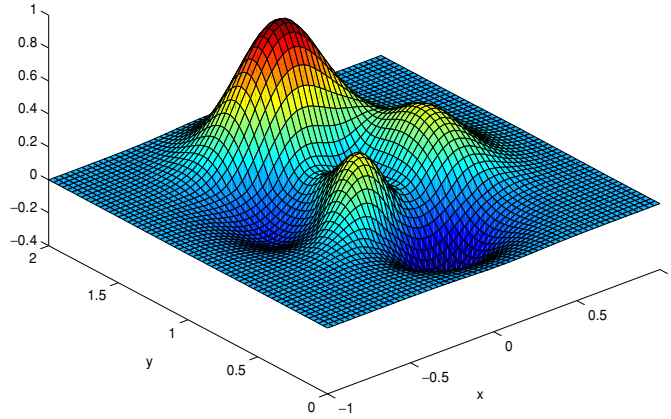
Figure 2. Example 1: true scatterer q_1.

or in short

$$A_i q = f_i, \qquad i = 1, \ldots, I.$$

For each sweep i, the Landweber iteration takes the form

$$q_i^{(l)} = q_i^{(l-1)} + \alpha A_i^* \left(f_i - A\left(q_i^{(l-1)}\right) \right), \qquad l \in \mathbb{N},$$

where α is a relaxation parameter. Since we just need an initial guess for the iteration in the recursive linearization, we only take one step Landweber iteration for each sweep, which yields

$$q_i = q_{i-1} + \alpha A_i^* (f_i - A(q_{i-1})), \qquad i = 1, \ldots, I, \tag{3.5}$$

where q_I is used as the starting point of the following recursive linearization algorithm.

3.2. Recursive linearization

As discussed in the previous section, when the spatial frequency $|\eta|$ is large, the Born approximation allows a reconstruction of the thin layer for the true scatterer. In this section, a regularized recursive linearization method for solving the two-dimensional Helmholtz equation at fixed frequency is proposed.

Choose a large positive number $\eta_{\max}$ and divide the interval $[0, \eta_{\max}]$ into N subdivisions with the endpoints $\{\eta_0, \eta_1, \ldots, \eta_N\}$, where $\eta_0 = 0$, $\eta_N = \eta_{\max}$ and $\eta_{i-1} < \eta_i$ for $1 \leqslant i \leqslant N$. We intend to obtain q_η recursively at $\eta = \eta_N, \eta_{N-1}, \ldots, \eta_0$.

Suppose now that the scatterer $q_{\tilde{\eta}}$ has been recovered at some $\tilde{\eta} = \eta_{i+1}$ and that $\eta = \eta_i$ is slightly less than $\tilde{\eta}$. We wish to determine q_η, or equivalently, to determine the perturbation

$$\delta q = q_\eta - q_{\tilde{\eta}}.$$

For the reconstructed scatterer $q_{\tilde{\eta}}$, we solve at the spatial frequency η the forward scattering problem

$$\Delta \tilde{\psi}^{(j,i)} + k_0^2 (1 + q_{\tilde{\eta}}) \tilde{\psi}^{(j,i)} = -k_0^2 q_{\tilde{\eta}} \phi_0^{(j,i)}, \tag{3.6}$$

$$\frac{\partial \tilde{\psi}^{(j,i)}}{\partial n} - i k_0 \tilde{\psi}^{(j,i)} = 0, \tag{3.7}$$
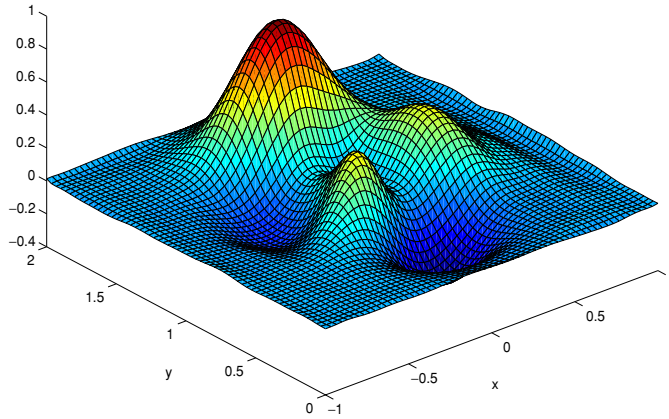
Figure 3. Example 1: final reconstruction q_1.

Table 1. Recursive linearization reconstruction algorithm.

Initialization
    $\eta_N = \eta_{max}$ largest η_{max}
    $q_{\eta_{max}}$ Born approximation
Reconstruction loop:
    FOR $i = N : 0\,(\eta_i = \eta_{max} : \eta_0)$ march along spatial frequency
        FOR $j = N : i\,(|\eta_j| = \eta_{max} : \eta_i)$ perform refinement
            solve (3.6), (3.7) for $\tilde{\psi}^{(j,i)}$ one forward problem
            solve (3.17), (3.18) for $\phi^{(j,i)}$ one adjoint problem
            $\delta q_i^j = k_0^2 \beta (\overline{\phi_0^{(j,i)} + \tilde{\psi}^{(j,i)}}) \phi^{(j,i)}$
            $q_i^j := q_i^j + \delta q_i^j$
        END
        $q_i := q_i^i$
    END
    $q := q_0$ final reconstruction

where the incident wave

$$\phi_0^{(j,i)} = \exp(i\eta_j x_1 + ik(\eta_j)x_2), \qquad |j| \geqslant i.$$

For the scatterer q_η, we have

$$\Delta \psi^{(j,i)} + k_0^2 (1 + q_\eta)\psi^{(j,i)} = -k_0^2 q_\eta \phi_0^{(j,i)}, \tag{3.8}$$

$$\frac{\partial \psi^{(j,i)}}{\partial n} - ik_0 \psi^{(j,i)} = 0. \tag{3.9}$$

Subtracting (3.6), (3.7) from (3.8), (3.9) and omitting the second-order smallness in δq and in $\delta \psi^{(j)} = \psi^{(j,i)} - \tilde{\psi}^{(j,i)}$, we obtain

$$\Delta \delta \psi^{(j)} + k_0^2 (1 + q_{\tilde{\eta}})\delta \psi^{(j)} = -k_0^2 \delta q \left(\phi_0^{(j,i)} + \tilde{\psi}^{(j,i)} \right), \tag{3.10}$$

$$\frac{\partial \delta \psi^{(j)}}{\partial n} - ik_0 \delta \psi^{(j)} = 0. \tag{3.11}$$
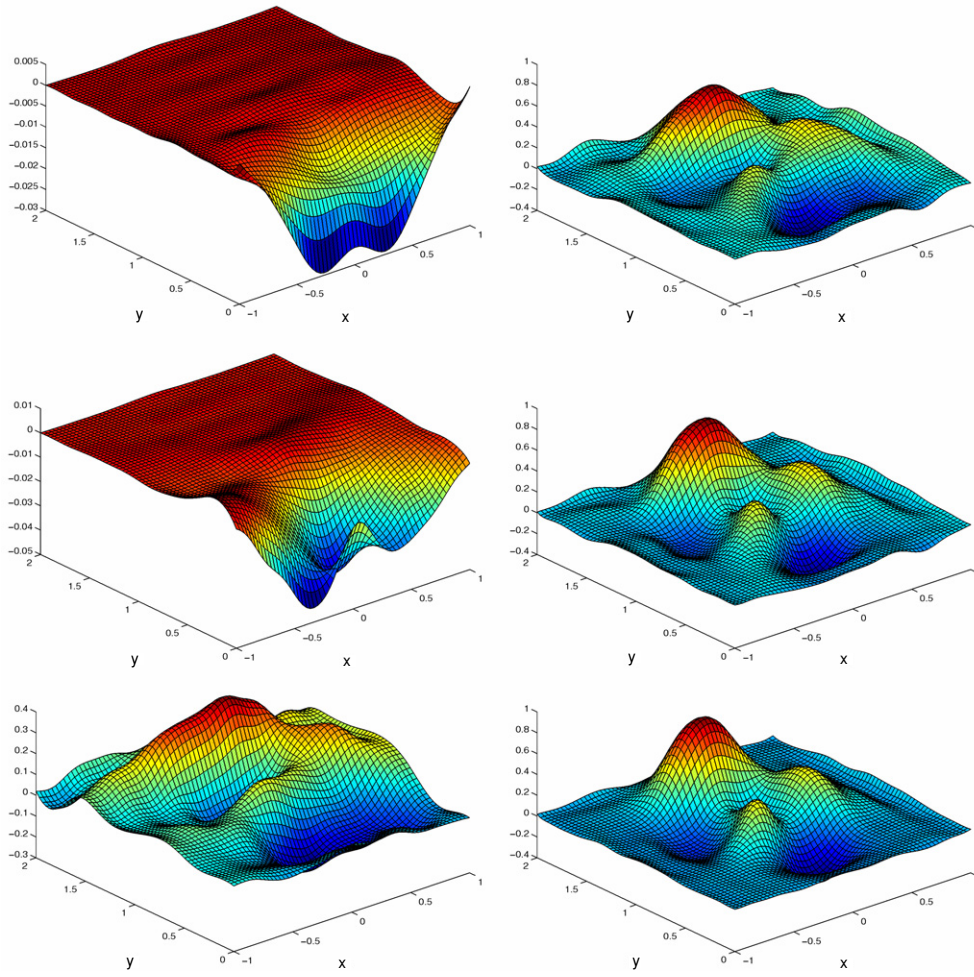
Figure 4. Example 1: evolution of the reconstruction q_1. Left column from top to bottom: Born approximation; reconstruction at $\eta = 10.2$; reconstruction at $\eta = 8.4$; right column from top to bottom: reconstruction at $\eta = 6.6$; reconstruction at $\eta = 4.8$; reconstruction at $\eta = 3.0$.

For the scatterer q_η and the incident wave $\phi_0^{(j,i)}$, we define the map $S_j\big(q_\eta, \phi_0^{(j,i)}\big)$ by

$$S_j\big(q_\eta, \phi_0^{(j,i)}\big) = \psi^{(j,i)},$$

where $\psi^{(j,i)}$ is the scattering data corresponding to the incident wave $\phi_0^{(j,i)}$. Let γ be the trace operator to the boundary ∂D. Define the scattering map

$$M_j\big(q_\eta, \phi_0^{(j,i)}\big) = \gamma S_j\big(q_\eta, \phi_0^{(j,i)}\big).$$

For simplicity, denote $M_j\big(q_\eta, \phi_0^{(j,i)}\big)$ by $M_j(q_\eta)$. By the definition of the trace operator, we have

$$M_j(q_\eta) = \psi^{(j,i)}|_{\partial D}.$$

Let $DM_j(q_{\tilde{\eta}})$ be the Fréchet derivative of $M_j(q_\eta)$ and denote the residual operator by

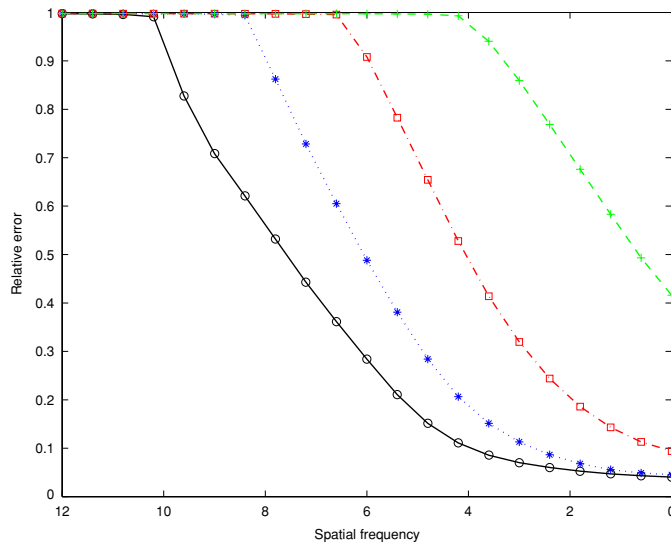$$R_j(q_{\tilde{\eta}}) = \psi^{(j,i)}|_{\partial D} - \tilde{\psi}^{(j,i)}|_{\partial D}.$$

Figure 5. Example 1: relative error of the reconstruction q_1 at different wavenumbers k_0. ($\circ$) reconstruction at $k_0 = 10.0$; ($*$) reconstruction at $k_0 = 8.0$; ($\square$) reconstruction at $k_0 = 6.0$; (+) reconstruction at $k_0 = 4.0$.
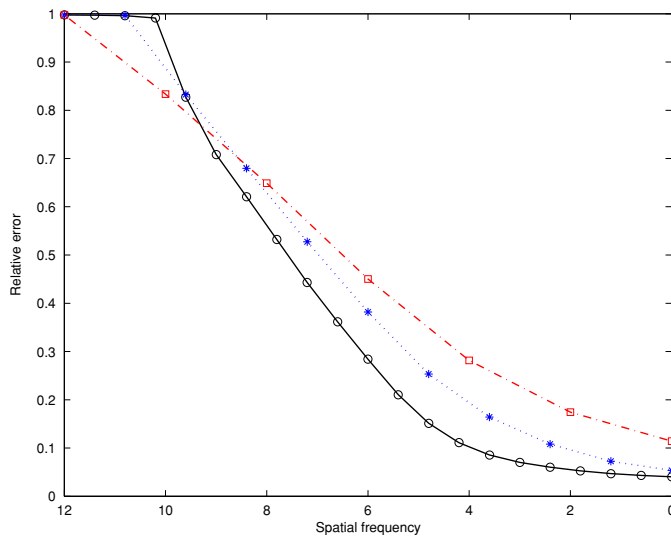

Figure 6. Example 1: relative error of the reconstruction q_1 at different step sizes $\delta\eta$. ($\circ$) reconstruction at $\delta\eta = 0.6$; ($*$) reconstruction at $\delta\eta = 1.2$; ($\square$) reconstruction at $\delta\eta = 2.0$.

It follows from theorem 2.1 that

$$DM_j(q_{\tilde{\eta}})\delta q = R_j(q_{\tilde{\eta}}). \tag{3.12}$$

Similarly, in order to reduce the computation cost and instability, we consider the Landweber iteration of (3.12), which has the form

$$\delta q = \beta DM_j^*(q_{\tilde{\eta}})R_j(q_{\tilde{\eta}}), \qquad \text{for all} \quad |j| \geqslant i, \tag{3.13}$$
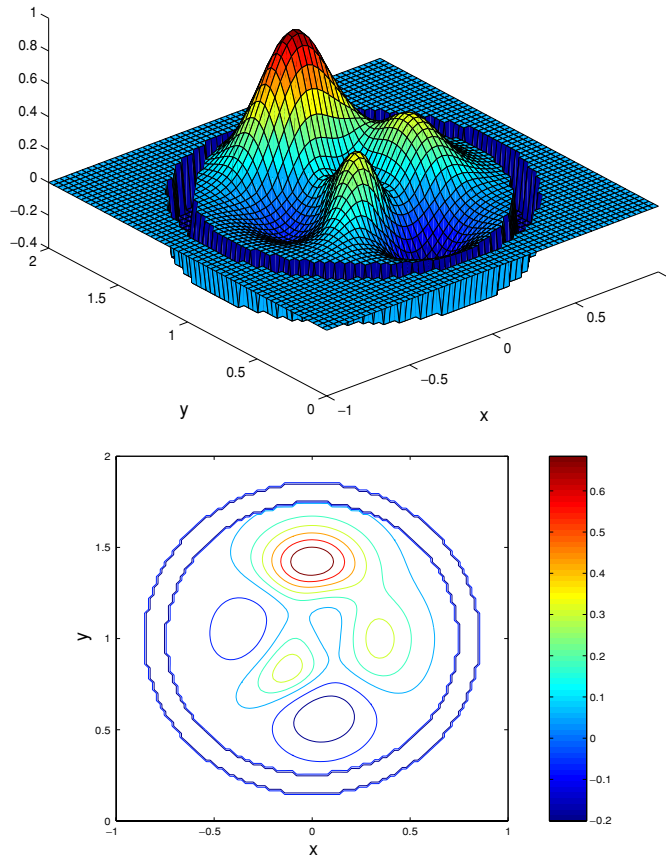
Figure 7. Example 2: surface and contour views of the true scatterer q_2.

where β is a relaxation parameter and $DM_j^*(q_{\tilde{\eta}})$ is the adjoint operator of $DM_j(q_{\tilde{\eta}})$.

In order to compute the correction δq, we need some efficient way to compute $DM_j^*(q_{\tilde{\eta}})R_j(q_{\tilde{\eta}})$, which is given by the following theorem.

Theorem 3.1. *Given residual $R_j(q_{\tilde{\eta}})$, there exits a function $\phi^{(j,i)}$ such that the adjoint Fréchet derivative $DM_j^*(q_{\tilde{\eta}})$ satisfies*

$$[DM_j^*(q_{\tilde{\eta}})R_j(q_{\tilde{\eta}})](x) = k_0^2\big(\overline{\phi_0^{(j,i)}}(x) + \overline{\tilde{\psi}^{(j,i)}}(x)\big)\phi^{(j,i)}(x), \tag{3.14}$$

where $\phi_0^{(j,i)}$ is the incident wave and $\tilde{\psi}^{(j,i)}$ is the solution of (3.6), (3.7) with the incident wave $\phi_0^{(j,i)}$.

Proof. Let $\tilde{\psi}^{(j,i)}$ be the solution of (3.6), (3.7) with the incident wave $\phi_0^{(j,i)}$. Consider the following problem:

$$\Delta\delta\psi^{(j)} + k_0^2(1 + q_{\tilde{\eta}})\delta\psi^{(j)} = -k_0^2\delta q\big(\phi_0^{(j,i)} + \tilde{\psi}^{(j,i)}\big), \tag{3.15}$$

$$\frac{\partial\delta\psi^{(j)}}{\partial n} - ik_0\delta\psi^{(j)} = 0, \tag{3.16}$$

and the adjoint problem

$$\Delta\phi^{(j,i)} + k_0^2(1 + q_{\tilde{\eta}})\phi^{(j,i)} = 0, \tag{3.17}$$

$$\frac{\partial\phi^{(j,i)}}{\partial n} + \mathrm{i}k_0\phi^{(j,i)} = R_j(q_{\tilde{\eta}}). \tag{3.18}$$

Since the existence and uniqueness of the weak solution for the adjoint problem may be established by following the same proof of lemma 2.2, we omit the proof here.

Multiplying equation (3.15) with the complex conjugate of $\phi^{(j,i)}$ and integrating over D on both sides, we obtain

$$\int_D \overline{\phi^{(j,i)}}\Delta\delta\psi^{(j)}\,\mathrm{d}x + k_0^2\int_D(1 + q_{\tilde{\eta}})\delta\psi^{(j)}\overline{\phi^{(j,i)}}\,\mathrm{d}x = -k_0^2\int_D \delta q\big(\phi_0^{(j,i)} + \tilde{\psi}^{(j,i)}\big)\overline{\phi^{(j,i)}}\,\mathrm{d}x.$$

Integration by parts yields

$$\int_{\partial D}\left(\overline{\phi^{(j,i)}}\frac{\partial\delta\psi^{(j)}}{\partial n} - \delta\psi^{(j)}\frac{\overline{\partial\phi^{(j,i)}}}{\partial n}\right)\mathrm{d}s = -k_0^2\int_D \delta q\big(\phi_0^{(j,i)} + \tilde{\psi}^{(j,i)}\big)\overline{\phi^{(j,i)}}\,\mathrm{d}x.$$

Using the boundary condition (3.16), we deduce

$$\int_{\partial D}\delta\psi^{(j)}\left(\frac{\overline{\partial\phi^{(j,i)}}}{\partial n} - \mathrm{i}k_0\overline{\phi^{(j,i)}}\right)\mathrm{d}s = k_0^2\int_D \delta q\big(\phi_0^{(j,i)} + \tilde{\psi}^{(j,i)}\big)\overline{\phi^{(j,i)}}\,\mathrm{d}x.$$

It follows from (3.12) and the boundary condition (3.18) that

$$\int_{\partial D}[DM_j(q_{\tilde{\eta}})\delta q]\overline{R_j(q_{\tilde{\eta}})}\,\mathrm{d}s = k_0^2\int_D \delta q\big(\phi_0^{(j,i)} + \tilde{\psi}^{(j,i)}\big)\overline{\phi^{(j,i)}}\,\mathrm{d}x.$$

We know from the adjoint operator $DM_j^*(q_{\tilde{\eta}})$ that

$$\int_D \delta q\,\overline{DM_j^*(q_{\tilde{\eta}})R_j(q_{\tilde{\eta}})}\,\mathrm{d}x = k_0^2\int_D \delta q\big(\phi_0^{(j,i)} + \tilde{\psi}^{(j,i)}\big)\overline{\phi^{(j,i)}}\,\mathrm{d}x.$$

Since it holds for any δq, we have

$$\overline{DM_j^*(q_{\tilde{\eta}})R_j(q_{\tilde{\eta}})} = k_0^2\big(\phi_0^{(j,i)} + \tilde{\psi}^{(j,i)}\big)\overline{\phi^{(j,i)}}.$$

Taking the complex conjugate of the above equation yields the result. □

Using this theorem, we can rewrite (3.13) as

$$\delta q = k_0^2\beta\big(\overline{\phi_0^{(j,i)}} + \overline{\tilde{\psi}^{(j,i)}}\big)\phi^{(j,i)}. \tag{3.19}$$

So for each incident wave with a transverse part η_j, we have to solve one forward problem (3.6), (3.7) along with one adjoint problem (3.17), (3.18). Since the adjoint problem has a similar variational form as the forward problem. Essentially, we need to compute two forward problems at each sweep. Once δq is determined, $q_{\tilde{\eta}}$ is updated by $q_{\tilde{\eta}} + \delta q$. After completing sweeps with $|\eta_j| \geqslant \eta$, we get the reconstructed scatterer q_η at the spatial frequency η.

Remark 3.1. For given η_i, iterations for $|\eta_j| \geqslant \eta_i$ could be repeated to improve the accuracy of the approximation for q_{η_i}. However, in practice, this refinement is usually unnecessary because of the slow convergence of the Landweber iteration at the same stage [11], i.e., without using essentially different data. Numerical results show that the iterative process described as the reconstruction loop in table 1 is sufficient to obtain reasonable accuracy.

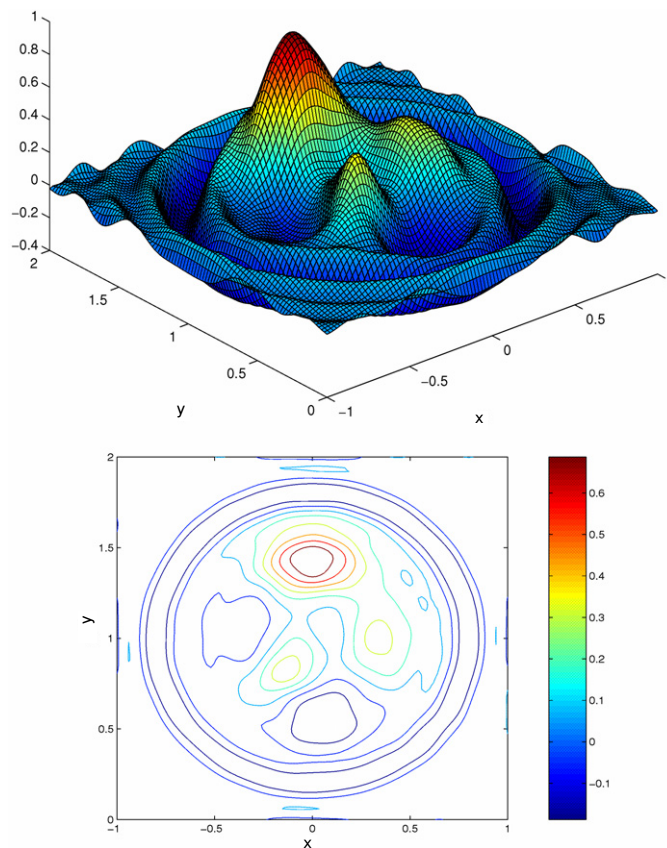The recursive linearization for inverse medium scattering at fixed frequency is summarized in table 1.

Figure 8. Example 2: surface and contour views of the reconstructed scatterer q_2.

4. Numerical experiments

In this section, we discuss the numerical solution of the forward scattering problem and the computational issues of the recursive linearization algorithm.

The scattering data are obtained by numerical solution of the forward scattering problem. As for the forward solver, we adopt the finite element method (FEM), which leads to a sparse matrix. The sparse large-scale linear system can be most efficiently solved if the zero elements of coefficient matrix are not stored. We used the commonly used compressed row storage (CRS) format which makes no assumptions about the sparsity structure of the matrix and does not store any unnecessary elements. In fact, from the variational formula of our direct problem (2.1), the coefficient matrix is complex symmetric. Hence, only the lower triangular portion of the matrix needs be stored. Regarding the linear solver, either BiConjugate gradient (BiCG) or quasi-minimal residual (QMR) algorithms with diagonal preconditioning may be used to solve the sparse, symmetric and complex system of the equations. For our examples, it appears that the QMR is more efficient.

In the following, to illustrate the performance of the algorithm, three numerical examples are presented for reconstructing the scatterer of the Helmholtz equation in two dimensions.
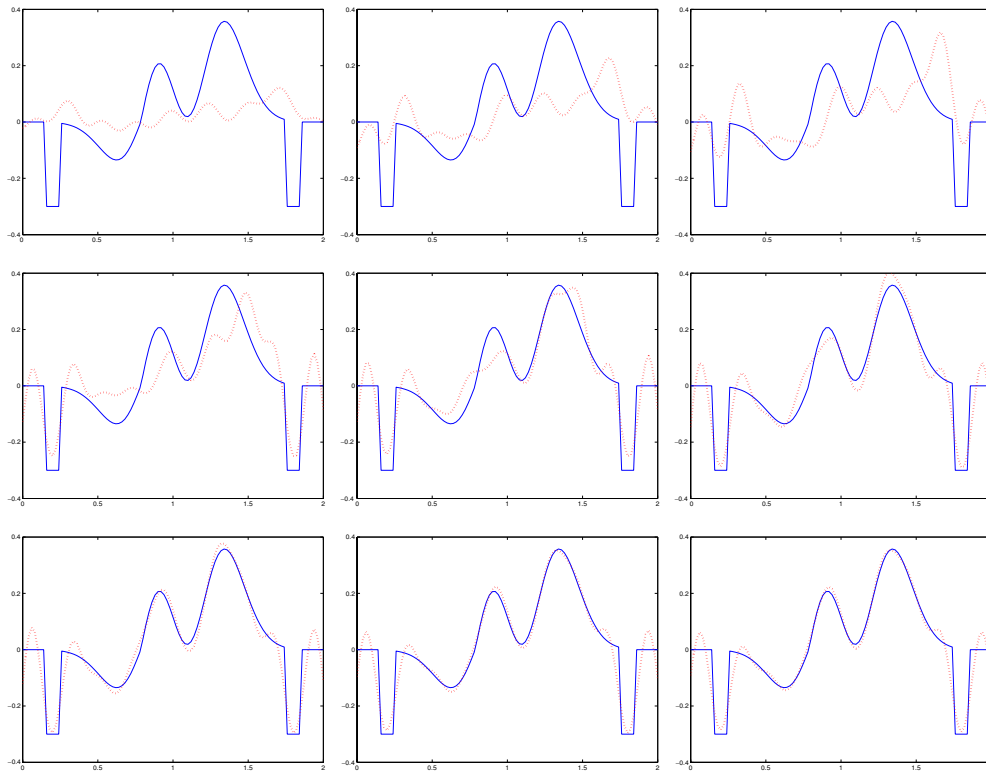
Figure 9. Example 2: evolution of slice for the reconstruction q_2. Solid line: true scatterer; dotted line: reconstruction. Top row from left to right: reconstruction at $\eta = 14.45$; reconstruction at $\eta = 13.60$; reconstruction at $\eta = 12.75$; middle row from left to right: reconstruction at $\eta = 10.20$; reconstruction at $\eta = 8.50$; reconstruction at $\eta = 6.80$; bottom row from left to right: reconstruction at $\eta = 5.10$; reconstruction at $\eta = 2.55$; reconstruction at $\eta = 0.0$.

For stability analysis, some relative random noise is added to the date, i.e., the electric field takes the form

$$\psi|_{\partial D} := (1 + \sigma \, \mathrm{rand}) \psi|_{\partial D}.$$

Here, rand gives uniformly distributed random numbers in $[-1, 1]$ and σ is a noise level parameter taken to be 0.02 in our numerical experiments. The relaxation parameter β is taken to be 0.01. Define the relative error by

$$e_2 = \frac{\left(\sum_{i,j} |q_{ij} - \bar{q}_{ij}|^2 \right)^{\frac{1}{2}}}{\left(\sum_{i,j} |q_{ij}|^2 \right)^{\frac{1}{2}}},$$

where $\bar{q}$ is the reconstructed scatter and q is the true scatterer.

Example 1. Let

$$q(x_1, x_2) = 0.3(1 - x_1)^2 \exp\left(-x_1^2 - (x_2 + 1)^2\right) - \left(\frac{x_1}{5} - x_1^3 - x_2^5\right) \exp\left(-\left(x_1^2 + x_2^2\right)\right)$$

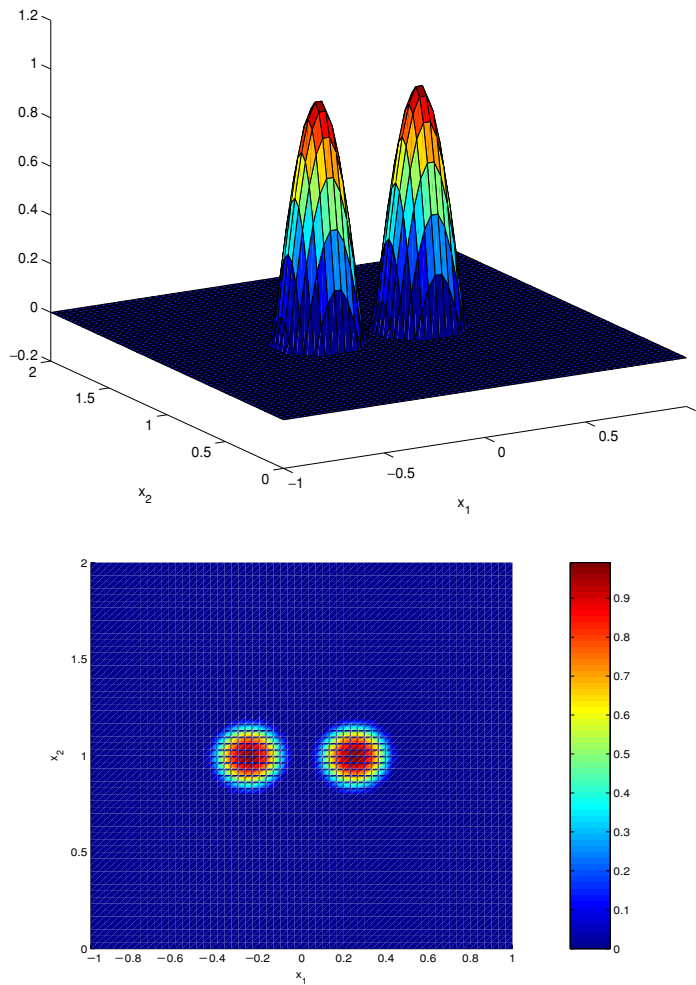$$- \frac{1}{30} \exp\left(-(x_1 + 1)^2 - x_2^2\right)$$

Figure 10. Example 3: surface and image views of the true scatterer q_3.

reconstruct a scatterer defined by

$$q_1(x_1, x_2) = q(3x_1, 3(x_2 - 1)) \tag{4.1}$$

inside the domain $D = [-1, 1] \times [0, 2]$. See figure 2 for the surface plot of the scatterer function. Figure 3 is the final reconstruction using the wavenumber $k_0 = 10.0$ and the step size of the spatial frequency $\delta\eta = 0.6$. Figure 4 shows the evolution of reconstructions at different spatial frequencies. Figure 5 presents the effect of the wavenumber k_0 on the result of reconstruction, which illustrates clearly that the inversion using a larger wavenumber k_0 is better than that using a smaller one. This result may be explained by Heisenberg's uncertainty principle [6, 7]. Figure 6 shows the relative error by using different step sizes of the spatial frequency, which suggests that we may use a large step size in order to save computation cost since the final reconstruction is not really sensitive to the step size.
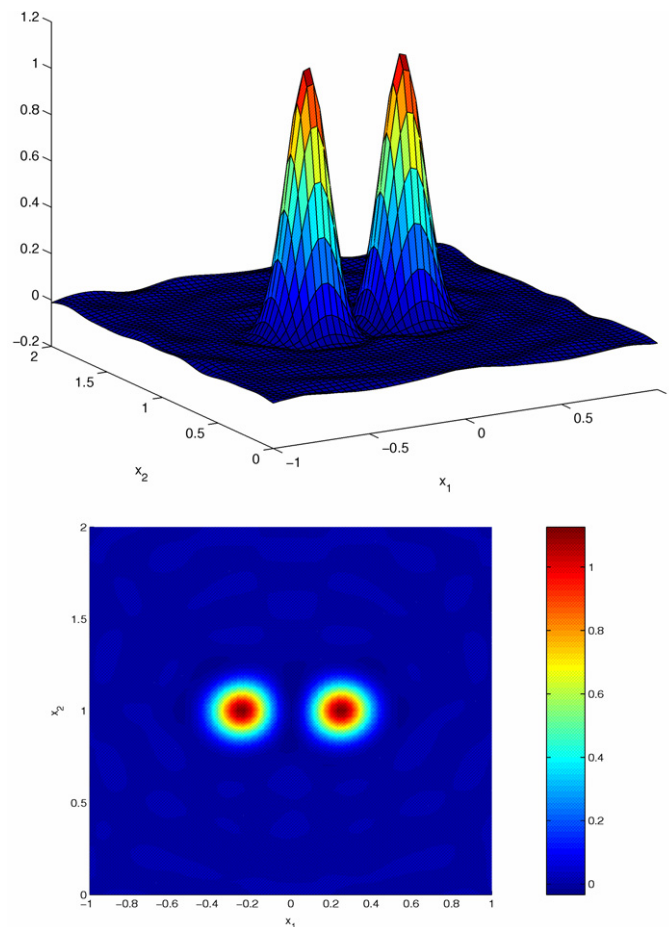
Figure 11. Example 3: surface and image views of the reconstructed scatterer q_3.

Example 2. Reconstruct a scatterer defined in D by

$$q_2(x_1, x_2) = \begin{cases} q_1(x_1/0.8, x_2/0.8), & \text{for} \quad x_1^2 + (x_2 - 1)^2 \leqslant 0.747^2, \\ -0.3, & \text{for} \quad 0.747^2 < x_1^2 + (x_2 - 1)^2 \leqslant 0.853^2, \\ 0, & \text{for} \quad x_1^2 + (x_2 - 1)^2 > 0.853^2. \end{cases}$$

See figure 7 for the surface and contour plots of the function. It is easily seen that this scatterer is difficult to reconstruct because of the discontinuity across two circles. The example could be regarded as a model problem for ultrasound tomography of a human head, where the skull is represented by the thin layer of denser material in the narrow annulus region. Figure 8 shows the surface and contour plots of the reconstructed scatterer using the wavenumber $k_0 = 15.0$ and the step size $\delta\eta = 0.85$. Figure 9 gives the evolution of reconstruction horizontally across the diameter. An examination of the plots shows that the error of the reconstructions occurs largely around the discontinuities, while the smooth part is recovered more accurately. As expected, the Gibbs phenomenon appears in the reconstructed scatterer near the discontinuity.

Example 3. Reconstruct a scatterer defined in D by

$$q_3(x_1, x_2) = \begin{cases} \cos(2.5\pi r_1), & \text{for} \quad r_1 \leqslant 0.2, \\ \cos(2.5\pi r_2), & \text{for} \quad r_2 \leqslant 0.2, \\ 0, & \text{otherwise}, \end{cases}$$

where $r_1 = \sqrt{(x_1 + 0.25)^2 + (x_2 - 1.0)^2}$ and $r_2 = \sqrt{(x_1 - 0.25)^2 + (x_2 - 1.0)^2}$. The compact support of this scatterer is two isolated discs with the same radius of 0.2 and the centres at $(-0.25, 1.0)$ and $(0.25, 1.0)$. See figure 10 for the surface plot and image of the function. Figure 11 is the final reconstruction using the wavenumber $k_0 = 3\pi$ and the step size of the spatial frequency $\delta\eta = 0.6$. This example is used to examine the resolution of the reconstructed image. In this numerical experiment, the wavelength of the incident plane waves is $2\pi/k_0 = 0.\dot{6}$. The distance of the centres for the compact support is 0.5, which is less than one wavelength. From the well-separated bumps, the resolution of the image is clearly in the scale of subwavelength. The subwavelength resolution is expected since evanescent waves are used for illumination.

5. Concluding remarks

We have presented a new continuation method with respect to the spatial frequency of a one-parameter family of plane waves. The recursive linearization algorithm is robust and efficient for solving the inverse medium scattering at fixed frequency. Finally, we point out some future directions along the line of this work. The first is concerned with the convergence analysis. Although our numerical experiments demonstrate the convergence and stability of the inversion algorithm, no rigorous mathematical result is available at present. Another direction is to investigate inverse medium problems for Maxwell's equations at fixed frequency. We are currently attempting to extend the approach in this paper to the more complicated 3D model problems and will report the progress elsewhere.

Acknowledgment

References

[1] Bao G, Chen Y and Ma F 2000 Regularity and stability for the scattering map of a linearized inverse medium problem *J. Math. Anal. Appl.* **247** 255–71
[2] Bao G and Liu J 2003 Numerical solution of inverse problems with multi-experimental limited aperture data *SIAM J. Sci. Comput.* **25** 1102–17
[3] Bao G and Li P 2005 Inverse medium scattering problems for electromagnetic waves *SIAM J. Appl. Math.* **65** 2049–66
[4] Carney P and Schotland J 2001 Three-dimensional total internal reflection microscopy *Opt. Lett.* **26** 1072–4
[5] Carney P and Schotland J 2003 Near-field tomography *MSRI Ser. Math. Appl.* **47** 131–66
[6] Chen Y 1997 Inverse scattering via Heisenberg uncertainty principle *Inverse Problems* **13** 253–82
[7] Chen Y 1997 Inverse scattering via skin effect *Inverse Problems* **13** 649–67
[8] Colton D and Kress R 1998 *Inverse Acoustic and Electromagnetic Scattering Theory* 2nd edn (Berlin: Springer) *Appl. Math. Sci.* **93**
[9] Courjon D 2003 *Near-Field Microscopy and Near-Field Optics* (London: Imperial College Press)

[10] Courjon D and Bainier C 1994 Near field microscopy and near field optics *Rep. Prog. Phys.* **57** 989–1028
[11] Engl H, Hanke M and Neubauer A 1996 *Regularization of Inverse Problems* (Dordrecht: Kluwer)
[12] Gilbarg D and Trudinger N 1983 *Elliptic Partial Differential Equations of Second Order* (New York: Springer)
[13] Girard C and Dereux A 1996 Near-field optics theories *Rep. Prog. Phys.* **59** 657–99
[14] Jerison D and Kenig C 1985 Unique continuation and absence of positive eigenvalues for Schrödinger operators *Ann. Math.* **121** 463–88
[15] Jin J 2002 *The Finite Element Methods in Electromagnetics* (New York: Wiley)
[16] Keys R G and Weglein A B 1983 Generalized linear inversion and the first born theory for acoustic media *J. Math. Phys.* **24** 1444–9
[17] Natterer F 1986 *The Mathematics of Computerized Tomography* (Stuttgart: Teubner)
[18] Natterer F and Wübbeling F 1995 A propagation–backpropagation method for ultrasound tomography *Inverse Problems* **11** 1225–32